Measuring forest structure along productivity gradients in the Canadian boreal with small-footprint Lidar

Douglas K. Bolton

Integrated Remote Sensing Studio, Department of Forest Resources Management, Faculty of Forestry, University of British Columbia, 2424 Main Mall, Vancouver, British Columbia, V6T 1Z4, Canada

Tel. 604-822-6592

Fax. 604-822-9106

Email. doug.k.bolton@alumni.ubc.ca

Nicholas C. Coops

Integrated Remote Sensing Studio, Department of Forest Resources Management, Faculty of Forestry, University of British Columbia, 2424 Main Mall, Vancouver, British Columbia, V6T 1Z4, Canada

Michael A. Wulder

Canadian Forest Service (Pacific Forestry Centre), Natural Resources Canada, 506 West Burnside Road, Victoria, British Columbia, V8Z 1M5, Canada

Pre-print of published version.

Reference:

Bolton, D.K., N.C. Coops, and M.A. Wulder. (2013). Measuring forest structure along productivity gradients in the Canadian boreal with small-footprint Lidar. Environmental Monitoring and Assessment. Vol. 185, No. 8, Page 6617-6634.

DOI.

DOI: http://dx.doi.org/10.1007/s10661-012-3051-9

Abstract

The structure and productivity of boreal forests are key components of the global carbon cycle and impact the resources and habitats available for species. With this research we characterized the relationship between measurements of forest structure and satellite-derived estimates of gross primary production (GPP) over the Canadian boreal. We acquired stand level indicators of canopy cover, canopy height and structural complexity from nearly 25,000 km of small-footprint discrete return Light Detection and Ranging (Lidar) data and compared these attributes to GPP estimates derived from the MODerate resolution Imaging Spectroradiometer (MODIS). While limited in our capacity to control for stand age, we removed recently disturbed and managed forests using information on fire history, roads and anthropogenic change. We found that MODIS GPP was strongly linked to Lidar-derived canopy cover ($r = 0.74$, $p < 0.01$), however was only weakly related to Lidar-derived canopy height and structural complexity, as these attributes are largely a function of stand age. A relationship was apparent between MODIS GPP and the maximum sampled heights derived from Lidar, as growth rates and resource availability likely limit tree height in the prolonged absence of disturbance. The most structurally complex stands, as measured by the coefficient of variation of Lidar return heights, occurred where MODIS GPP was highest, as productive boreal stands are expected to contain a wider range of tree heights and transition to uneven-aged structures faster than less productive stands. While MODIS GPP related near-linearly to Lidar-derived canopy cover, the weaker relationships to Lidar-derived canopy height and structural complexity highlight the importance of stand age in determining the structure of boreal forests. We conclude that an improved quantification of how both productivity and disturbance shape stand structure is needed to better understand the current state of boreal forests in Canada and how these forests are changing in response to changing climate and disturbance regimes.

Keywords

Forest structure, Productivity, Lidar, Remote Sensing, Boreal

1. Introduction

The three-dimensional structure of forests is an important indicator of biodiversity and carbon dynamics in terrestrial ecosystems (McElhinny et al. 2005; Fahey et al. 2010). Forests with a variety of structural components likely provide a wide range of habitats and resources for species (McElhinny et al. 2005), resulting in a positive correlation between the structural complexity of forests and biodiversity (Mac Nally et al. 2001; Tanabe et al. 2001). In addition, the structure of forests is an integral part of the global carbon cycle as tree volume and density determine above-ground carbon storage (Houghton et al. 2009) and foliage amounts drive the sequestration of carbon from the atmosphere into the terrestrial biosphere (Schulze et al. 2002).

Of the estimated 861 ± 66 petagrams of carbon stored in forests, 32% is reported to be stored in the boreal (Pan et al. 2011). In addition to containing a large portion of the world's forests, the boreal is expected to be among the biomes most impacted by a changing climate (Parry et al. 2007). To accurately forecast how climate change will affect biodiversity and carbon dynamics in boreal ecosystems, we require an improved quantification of the natural and anthropogenic factors that control boreal forest structure and how these factors are changing. Disturbance, site productivity, species composition, and forest management are the main drivers of structure in boreal forests (Spies 1998; Boucher et al. 2006; Boisvenue and Running 2006; Brassard and Chen 2006). In the northern boreal of Canada where most forests are not subject to management activities (Andrew et al. 2012), our knowledge of the impact of these factors on structure is limited by a lack of plots or inventory data (Gillis et al. 2005), preventing a clear understanding of how forest structure will be altered by a changing climate.

Disturbance, principally fire, is the dominant driver of stand age and structure in Canadian boreal forests (Kurz and Apps 1999; Bond-Lamberty et al. 2007; Amiro et al. 2009). The time between fires, known as the fire cycle, increases from west to east in the Canadian boreal and is controlled primarily by climate and the probability of lightning strikes (Brassard and Chen 2006). Approximately 2 million hectares of forests are burned annually in Canada (Stocks et al. 2002), with direct carbon emissions estimated to be an average of 27 Tg of carbon year^{-1} between 1959-1999 in Canada (Amiro et al. 2001). Stand-replacing fires release most of the carbon stored in above-ground biomass to the atmosphere while the time between fires impacts the accumulation of carbon back into a forest (Kasischke et al. 1995; Amiro et al. 2001). Forest stands generally transition through time from an even- to an uneven-aged structure (Brassard et al. 2008; Larson et al. 2008; Bradford and Kastendick 2010), resulting in stands becoming more structurally complex as time since fire increases. While fire is the dominant disturbance agent in boreal forests, non-stand-replacing disturbances, such as windthrow and insect outbreaks, are also critical to the formation of canopy gaps and lead to more structurally diverse forest stands (Brassard and Chen 2006, Chen and Popadiouk 2002). While localized insect outbreaks play a role in gap formation, regional outbreaks can have significant effects on forest structure and carbon dynamics. For instance, the current mountain pine beetle outbreak in British Columbia killed an estimated 692 million m^3 of mature merchantable pine between 1999 and 2010 (Walton 2011), converting the affected forests from a small carbon sink to a large carbon source (Kurz et al. 2008a). Projected range expansion of the mountain pine beetle into the boreal could lead increased disturbance levels in the boreal through the addition of a new disturbance agent (Safranyik et al. 2010).

Site productivity describes the capacity for growth and development within a stand and plays a critical role in determining forest structure between disturbance events (Boucher et al. 2006). Solar radiation, temperature, water availability and soil nutrient availability are the basic drivers of productivity; however, foliage amounts and light use-efficiency ultimately determine the rate at which carbon can be sequestered into vegetation (Schulze et al. 2002; Running et al. 2004; Boisvenue and Running 2006). Temperature is the main limiting factor to productivity across most of the Canadian boreal, with rates of photosynthesis and decomposition decreasing from the southern to northern boreal in response to decreasing temperature (Churkina and Running 1998). The latitudinal gradient in temperature results in a latitudinal gradient in productivity (Churkina and Running 1998), allowing southern boreal stands to accumulate more biomass between disturbance events than less productive stands further north. Forests have been found to reach an uneven-aged structure faster on higher productivity sites in the boreal (Boucher et al. 2006; Larson et al. 2008), suggesting that southern boreal stands will also become structurally complex sooner than northern boreal stands following a stand-replacing disturbance. In addition, insufficient resources at low productivity sites can restrict maximum tree dimensions, limiting tree size diversity and structural complexity (Boucher et al. 2006).

Thirdly, species composition impacts structure in boreal forests, as stand initiating deciduous species are often replaced over time by shade-tolerant coniferous species (Bergeron 2000; Brassard and Chen 2006; Taylor and Chen 2011). Paré and Bergeron (1995) found that total above-ground biomass along a chronosequence in Québec strongly correlated to the presence of *Populus tremuloides* (trembling aspen), as trembling aspen reached heights unmatched by other boreal species. Therefore, the transition from deciduous to coniferous dominance may be accompanied by a decrease in carbon storage where trembling aspen is in high abundance. The transition from deciduous to coniferous dominance can increase structural complexity with the development of multi-layered and multi-aged canopies, often accompanied by an increase in infestation by spruce budworm (Frelich and Reich 1995; Kneeshaw and Bergeron 1998). Canopy gaps formed by windthrow and insect outbreaks help maintain a deciduous component in older boreal stands (Taylor and Chen 2011), increasing the diversity of tree species and sizes. Older stands consisting purely of late successional conifers can be less structurally diverse than mixedwood stands that maintain a deciduous component (Paré and Bergeron 1995; Brassard et al. 2008), suggesting that structural complexity will not continuously increase with age.

Lastly, active management of forest resources impacts structure with between 700,000 to 1,000,000 ha of forests harvested annually in Canada over the past 20 years (Masek et al. 2011). Clear-cutting is the most common form of harvesting, where contiguous groups of trees are removed and carbon is transferred from above-ground biomass into the forestry sector (Kurz et al. 2009). In most managed forests where sufficient time has elapsed for a second harvest, the rotation time between clear-cuts is shorter than the natural fire cycle, preventing the development of uneven-aged structurally complex systems common in later stages of succession (Bergeron et al. 2004).

Increased fire frequency and intensity (Flannigan et al. 2005) as well as more favorable conditions for insect pests (Carroll et al. 2003; Safranyik et al. 2010) are projected for most Canadian boreal forests, potentially decreasing carbon storage (Thornley and Cannell 2004; Kurz et al. 2008b) and structural complexity (Kneeshaw and Gauthier 2003) in boreal forest ecosystems. Conversely, rising temperatures suggest increased productivity at high latitudes where precipitation is not a limiting factor (Boisvenue and Running 2006), which will likely increase the amount of carbon sequestrated and stored in boreal forests (Denman et al. 2007). While changes in productivity are expected to alter boreal forest structure, the cost and difficulty of collecting inventory data over large areas (Gillis et al. 2005; Wulder et al. 2007; Masek et al. 2011) has limited our quantification of the relationship between productivity and structure. To forecast the coupled effects of changing disturbance regimes and increased productivity on forest structure, the link between productivity and structure in the boreal must be better characterized.

Light Detection and Ranging (Lidar), an active remote sensing technology, provides an opportunity to characterize forest structure over larger spatial scales and at higher sampling frequencies than with conventional field methods (Dubayah and Drake 2000; Lefsky et al. 2002; Lim et al. 2003; Wulder et al. 2008a; Vierling et al. 2011). Lidar systems measure the distance to objects by emitting pulses of near-infrared laser energy and recording the timing and intensity of pulse returns (Wehr and Lohr 1999). The three-dimensional coordinates of objects are derived by coupling these distance measurements with global positioning systems and an inertial measurement unit (Wehr and Lohr 1999). When millions of Lidar pulses are emitted over forest canopies (e.g., >1 pulse/m^2), discrete return Lidar systems ultimately produce a cloud of points describing the structure of forest stands (Wehr and Lohr 1999; Lim et al. 2003). Most structural information in a Lidar point cloud can be summarized into three basic attributes: canopy height, canopy cover, and stand structural complexity (Lefsky et al. 2005; Kane et al. 2010b). Canopy height and cover can be estimated directly from a point cloud (Wulder et al. 2008a), while structural complexity can be inferred by the variation in point height (Zimble et al. 2003).

In this paper we investigate how forest structure across the Canadian boreal forest, as measured by Lidar remote sensing, relates to forest productivity, one of the key, yet poorly quantified, drivers of structure. We summarize the structure of forests using Lidar measures of canopy height, canopy cover and structural complexity for nearly 25,000 km of airborne Lidar data across the boreal, and compare these attributes to gross primary production (GPP) estimates from the MODerate-resolution Imaging Spectroradiometer (MODIS) and climate variables for six boreal ecozones. To reduce the impact of recent disturbance and management on the observed structure, we use information on land cover, fire history, anthropogenic change, and the presence of roads to restrict our study to mature unmanaged forest stands. Once stratified, we assess the relationship between MODIS GPP and Lidar-derived forest structure metrics across Canadian boreal forests.

2. Methods

2.1 Data sources

2.1.1 Lidar data

In the summer of 2010, the Canadian Forest Service (CFS) working with Applied Geomatics Research Group (AGRG) and the Canadian Consortium for LiDAR Environmental Applications Research (C-CLEAR) acquired 34 transects of small-footprint discrete return airborne Lidar data, spanning from Newfoundland in the east to the Yukon in the west (Wulder et al. 2012).

The 34 transects totaled 24,286 km in length with a minimum swath width of 400 m and a nominal pulse density of approximately 2.8 returns/m^2 (Fig. 1a). Data were collected using an Optech ALTM 3100 discrete return sensor between the altitudes of 450−1900 m with a fixed scan angle of 15º and a pulse repetition frequency of 70 kHz for most transects (Wulder et al. 2012). The average transect length was approximately 700 kilometers, largely determined by the location of suitable airports (for survey details see Hopkinson et al. 2011). Customized software tools were developed to pre-process the long transects of Lidar point data, including the classification of points into ground and non-ground returns (Hopkinson et al. 2011).

The Lidar dataset, which contains over 18 billion discrete return points, was divided into 25- by 25-m plots and a suite of Lidar metrics was calculated for each plot in FUSION (McGaughey 2012), a free software package produced by the US Forest Service for generating forest relevant metrics from Lidar data (Wulder et al. 2012). Lidar metrics describe the distribution and density of Lidar points within a point cloud, allowing plot-level point clouds to be summarized into relatively few structural metrics. Lefsky et al. (2005) and Kane et al. (2010b) found that most structural information in Lidar data could be summarized with a small set of metrics that describe the height, canopy cover, and structural complexity of forests. As a result of these findings, the 95th height percentile (canopy height), percentage of Lidar first returns above 2 m (canopy cover), and the coefficient of variation of return height (structural complexity) were selected as forest structure indicators.

Stand height

Height percentiles describe the cumulative height distribution of Lidar returns and correlate strongly to plot-level inventory attributes such as mean tree height, dominant tree height and stand volume (Wulder et al. 2008a). In Norway, Næsset (2004) explained 77-92% of the variation in Lorey's mean tree height using only height percentiles, while Wulder et al. (2012) explained 83% of the variation in Lorey's mean height in the Canadian boreal with the 95th height percentile alone. Here, the 95th height percentile was selected over the maximum return height or 99th height percentile as these latter metrics can provide unrepresentative estimates of stand height in the presence of physical (e.g., birds, power lines) or atmospheric anomalies (Magnussen and Boudewyn 1998; Kane et al. 2010b). The 95th percentile was calculated using only first returns above 2 m.

Canopy cover

Vegetation cover within any vertical position of a canopy can be estimated by calculating the ratio of Lidar pulses intercepted by a canopy layer to the total number of returns that entered the layer with well-established accuracy (Wulder et al. 2008a). Andersen (2009) used the percentage of first returns above 2 m to assess canopy closer in boreal Alaska while Solberg et al. (2006) used the percentage of returns above 1 m to assess insect defoliation in Norway. Likewise, Morsdorf et al (2006) found a strong correspondence (R^2 = 0.73) between Lidar and hemispherical photograph derived estimates of vegetation cover in Swiss mountain pine forests. Canopy cover was calculated as the ratio of first returns above 2 m to the total number of first returns, which conforms closely to most field definitions of canopy cover (Jennings et al. 1999; USDA Forest Service 2003).

Structural complexity

Lastly, the coefficient of variation (CV) of return height was selected as an indicator of stand structural complexity, as variability in return height within a forest canopy will relate to the variability of structural elements within the canopy. Zimble et al. (2003) found that single story canopies had a lower CV of return height than diverse multistory canopies in central Idaho forests. The standard deviation of return height tends to increase with stand height regardless of stand complexity (Kane et al. 2010a), making the CV a more useful index for comparing complexity across varying stand heights. While the 95th height percentile and cover above 2 m relate directly to easily measured components of a stand, the CV of return height serves only as an indicator of structural complexity, as complexity is difficult to define in the field. Therefore, the results should be interpreted with care. The CV was also calculated using first returns above 2 m.

These plot-level metrics, in addition to the other standard metrics calculated in FUSION, were stored in a PostgreSQL database (http://www.postgresql.org/; see Wulder et al. 2012 for a complete list of calculated metrics). From the over 18 billion Lidar points collected during the national transects campaign, Lidar metrics were generated for more than 17 million 25- by 25-m plots.

2.1.2 MODIS GPP

The MODIS GPP algorithm provides 8-day estimates of GPP globally at 1-km spatial resolution. Derived following the principles of Monteith (1972), GPP is determined for each 1-km cell as a function of the absorbed photosynthetically active radiation (APAR) and the light-use efficiency (LUE) of vegetation:

$$GPP = \varepsilon_{max} * 0.45 * SWrad * FPAR * fVPD * fT_{min}$$

where ε_{max} is the maximum LUE; SWrad is the incident short-wave solar radiation, multiplied by 0.45 to derive photosynthetically active radiation (PAR); FPAR is the fraction of incident PAR that is absorbed by vegetation; and fVPD and fT_{min} are reductions in LUE from high vapor pressure deficits (VPD) that lead to water stress in plants and low temperatures that limit plant function (Zhao and Running 2010).

The algorithm defines ε_{max} by vegetation type according to the MODIS Land Cover Type product (MOD12Q1, Friedl et al. 2010). Daily meteorological data is used to calculate minimum daily temperature (T_{min}), VPD and SWrad (Zhao and Running 2010). FPAR is determined using the 1-km MODIS FPAR product (MOD15A2, Myneni et al. 2011), which is computed from atmospherically corrected MODIS surface reflectances.

The MODIS GPP algorithm has been implemented in NASA's MOD17 product to provide 8-day and annual estimates of GPP from 2000-2011 (Running et al. 2004). Heinsch et al. (2006) showed that annual MODIS GPP (MOD17A3) had a relatively strong correlation to annual flux tower estimates of GPP across North America ($r = 0.859 \pm 0.173$), but overestimated the tower estimates at most sites (relative error = 24%). A re-processed version of MOD17A3, which addresses cloud and aerosol contamination issues (Zhao and Running 2010), was obtained for this analysis (available at: ftp://ftp.ntsg.umt.edu/pub/MODIS/Mirror/MOD17_Science_2010/). As inter-annual variability and temporal trends exist within these data (Zhao and Running 2010), GPP estimates from a single year are likely unrepresentative of long-term forest productivity. Therefore, the annual GPP products were compiled into a ten-year average (2001-2010), serving as a long-term estimate of productivity to relate to the Lidar-derived structural metrics. All processing in this analysis was then performed on the 1-km MODIS sinusoidal grid.

2.1.3 Climate data

Minimum annual temperature (MAT) and total annual precipitation (TAP) data for North America was obtained from the Pacific Climate Impacts Consortium (PCIC, http://pacificclimate.org/tools-and-data/datasets). These climate datasets were derived at 32-km spatial resolution from 1979-2010 by the National Centers for Environmental Prediction (NCEP) North American Regional Reanalysis (NARR) project (Mesinger et al. 2006). A natural neighbor interpolation approach was used to produce annual maps of MAT and TAP on the 1-km MODIS sinusoidal grid. The annual maps were averaged together to derive average MAT and TAP for 1979-2010.

2.1.4 Additional Datasets

Land cover was obtained from the Earth Observation for Sustainable Development of Forests (EOSD) program led by the CFS (Wulder et al. 2008b). The EOSD is a 25-m spatial resolution land cover classification of the forested ecozones of Canada derived from Landsat-7 Enhanced Thematic Mapper Plus (ETM+) images (circa 2000) and consists of 23 land cover classes, including 9 forest classes (coniferous, mixedwood and broadleaf / dense, open and sparse). These 9 forest classes were used to estimate the forested percentage of each 1-km MODIS cell (Fig. 1c). In addition, the 500 m MODIS Land Cover Type product (MOD12Q1, Friedl et al. 2010) was obtained from 2001-2010 to compare against the EOSD classification. All classes matching the EOSD definition of a forest (i.e., > 10% tree covered) according to the University of Maryland classification scheme (Friedl et al. 2010) were selected and used to calculate the forested percentage of each 1-km cell in each year.

Fire, road and anthropogenic disturbance layers were used to identify 1-km MODIS cells that potentially contained recent disturbances (Fig. 1d). The 2010 Canadian National Forest Database (CNFDB, Canadian Forest Service 2010) is a collection of fire polygons recorded by provincial and territorial fire management agencies and Parks Canada. While fire records in the CNFDB date back to 1917 in British Columbia, the oldest recorded fire to intersect a CFS Lidar transect was in 1941. The methods for recording fires have changed with time and vary by agency, ranging from sketches of fire boundaries to the interpretation of aerial photography and the classification of satellite imagery.

The 2010 Road Network File is a compilation of all Canadian roads recorded in Statistics Canada's National Geographic Database (Statistics Canada 2010). In this analysis, the Road Network File acts as an indicator of forest management: if a 1-km MODIS cell contains a road, then the forests within that cell are potentially managed. Logging roads that provide access to managed forests from existing roads may be absent from the Road Network File. Therefore, a 1-km cell was flagged as containing a road if one existed in a neighboring cell (3 by 3 cell window).

Lastly, Global Forest Watch Canada analyzed Landsat data (30-m spatial resolution) to produce anthropogenic change maps for areas in Nova Scotia (Cheng and Lee 2009), Saskatchewan and Manitoba (Stanojevic et al. 2006a), Ontario (Cheng and Lee 2008), Québec (Stanojevic et al. 2006b) and British Columbia (Lee and Gysbers 2008). The major anthropogenic changes identified and mapped in these studies include development, clear-cutting, road construction, agricultural clearing, reservoir construction and petroleum and natural gas exploration (Stanojevic et al. 2006b). The areas mapped by Global Forest Watch Canada do not cover the entire boreal, placing more importance on the Road Network File to identify potentially managed and anthropogenic disturbed forests. By combining the CNFBD, the Road Network File and the Global Forest Watch Canada's anthropogenic change layers, we are identifying, to the best of our ability, MODIS cells that contain recorded disturbance events or potentially managed forests.

Following the Canadian ecozone framework (Ecological Stratification Working Group 1995) and the Brandt definition of the boreal (Brandt 2009), six boreal ecozones were sampled and studied in this analysis (Fig. 1f). Because the Taiga and Boreal Shield ecozones are large and span a wide range of climatic and ecosystem conditions, both were split into east and west compartments (Stinson et al. 2011).

2.2 Selection of mature unmanaged forest cells

Indicators of canopy cover, canopy height and structural complexity were derived for each 1-km MODIS cell by averaging together the plot level (25- by 25-m) Lidar metrics within each cell. Only Lidar plots classified as forest by the EOSD and meeting the structural definition of a forest according to the 2005 Global Forest Resources Assessment (height [95th percentile] > 5 m, canopy cover [percent cover above 2 m] > 10%) were used to calculate the 1-km cell averages (Food and Agriculture Organization 2006). A "spatial uniqueness" test was performed on the Lidar plots to insure that no area was double counted in the MODIS cell averages where flight lines crossed. Lidar plots with a 95th height percentile above 50 m were assumed to be erroneous and were therefore removed prior to the calculation of the MODIS cell averages. In total, only 591 of 9.4 million forested Lidar plots had a 95th height percentile above 50 m.

MODIS cells containing less than 100 forested Lidar plots were removed from the analysis, in addition to cells where less than 75% of the Lidar plots were forested. MODIS cells that were less than 75% forested according to the EOSD (Fig. 1c) were also removed, as the GPP estimate could become unrepresentative of the forested portion of the cell with the presence of additional land covers. To remove the effects of disturbance and management on forest structure, cells that contained a fire, anthropogenic change or a road were also removed (Fig. 1d).

Given that vegetation type is a critical input to the MODIS GPP algorithm, misclassifications in the MODIS Land Cover Type product could result in less reliable GPP estimates (Zhao et al. 2005). Therefore, cells that were less than 75% forested in any year (2001-2010) according to the MODIS Land Cover Type product were also removed, as discrepancies between EOSD and MODIS land cover could signify incorrect vegetation inputs to the GPP calculation.

Averaging the 25- by 25-m plot metrics up to 1-km and applying this set of rules allowed for a direct comparison between Lidar structural metrics and MODIS GPP for mature unmanaged stands. Figure 1e shows the distribution of the 5675 MODIS cells that meet this set of rules (shaded by percent cover above 2 m), while Figure 1f shows the number of cells that fall within each boreal ecozone. The Boreal Shield East is of particular interest in this study because of its large sample size (1809) and large latitudinal gradient in GPP (Fig. 1b). The calculation of MODIS cell averages and the stratification of mature unmanaged stands was performed in R (R Development Core Team 2009).

2.3 Investigating the relationship between Lidar-derived structure and MODIS GPP

The relationship between Lidar-derived structural metrics and satellite-derived GPP was assessed using Pearson's correlation coefficient and the modified *t*-test proposed by Clifford et al. (1989) and altered by Dutilleul (1993). In the presence of positive spatial autocorrelation, a standard *t*-test is unfit for assessing the significance of a correlation coefficient as each sample does not constitute a full degree of freedom (Clifford et al. 1989). The modified t-test adjusts the degrees of freedom by calculating an "effective sample size" that is inversely proportional to the extent of spatial autocorrelation in each variable (full details can be found in Dutilleul 1993). To assess the extent of spatial autocorrelation, the distances between all pairs of points are divided into *k* distance strata and spatial autocorrelation is assessed for both variables in each strata. The specification of *k* impacts the calculation of the effective sample size as shorter distance intervals (i.e., larger value of *k*) will result in a higher calculated spatial autocorrelation (Fortin 1999) and a lower effective sample size. When relating wildfire and forest regeneration in Canadian boreal forests, Fortin and Payette (2002) found that the effective sample size increased as *k* decreased (i.e., larger distance interval), but decreasing *k* did not affect the acceptance or rejection of the null hypothesis. To assess the effect of *k* in this analysis, four distance intervals were tested in each ecozone: 5, 10, 20, and 40 km. The modified *t*-test was calculated for each ecozone using the Dutilleul (1993) modification in Pattern Analysis, Spatial Statistics and Geographic Exiegesis (PASSaGE), a freely available spatial analysis software package (Rosenberg and Anderson 2011). In addition to testing the relationship between Lidar-derived structure and MODIS GPP, the relationship between structure and the climate variables (i.e., MAT and TAP) was also assessed. Finally, linear regressions were developed in R to assess the slope of the relationships. We do not communicate the results of the analysis of the Taiga Shield West due to the small sample size in this ecozone (38 MODIS cells remained following stratification).

3. Results

3.1 Canopy cover

Table 1 presents the correlation coefficients (r), slopes and modified *t*-test results for the relationship between percent cover above 2 m and MODIS GPP, as well as both climate variables, using a distance interval of 10 km for the calculation of effective sample size. The number of strata (*k*) needed for a distance interval of 10 km varied from 84 in the Hudson Plains and Boreal Cordillera to 257 in the Boreal Shield East. The effective sample sizes were significantly smaller than the original sample sizes in all ecozones. While the Boreal Shield East has the most MODIS cells (1809), the effective sample sizes in the Boreal Shield East are among the smallest, with values between 11-13. The Boreal Shield West, Boreal Plains and Boreal Cordillera had the largest effective sample sizes, with each ecozone averaging > 50. The effective sample size increased as the distance interval increased from 5 to 40 km (results not shown), however this had no effect on the acceptance or rejection of the null hypothesis (α = 0.05). The level of significance did vary (i.e., from $p < 0.05$ to 0.01 or $p < 0.01$ to 0.001) in several cases when the distance interval was changed.

Figure 2 displays the relationship between percent cover above 2 m and MODIS GPP for each sampled ecozone as a series of boxplots. To investigate the differences between forest types, Figure 2a displays the relationship in the Boreal Shield East as a scatterplot, with points shaded by the dominant (> 50%) forest type within the cell according to the EOSD land cover classification. A statistically significant (α = 0.05) correlation between Lidar-derived canopy cover and MODIS GPP was found in all but the Hudson Plains, with the strongest link occurring in the Boreal Shield East (r = 0.74, p < 0.01, Fig. 2b). The correlation was weakest in the Boreal Shield West (r = 0.27, p < 0.05, Fig. 2c) and the Boreal Plains (r = 0.44, p < 0.01, Fig. 2d), both of which have a narrow sampled range in GPP. The link was strong between Lidar-derived canopy cover and MODIS GPP in the Boreal Cordillera (r = 0.58, p < 0.001, Fig. 2e) and the Taiga Plains (r = 0.70, p < 0.01, Fig. 2g), but the slope was shallower than in the Boreal Shield East. The sampled range in GPP was larger in the Boreal Shield East than in other ecozones, with a mean GPP value of less than 0.6 kgC $m^{-2}yr^{-1}$ for the 20 – 30 % cover group, increasing to over 1.0 kgC $m^{-2}yr^{-1}$ for the 80 – 90 % cover group. Markedly more stands had a canopy cover > 90% in the Boreal Shield East than in other ecozones and these stands had the highest mean GPP of all sampled cover groups (≈1.1 kgC $m^{-2}yr^{-1}$).

Figure 2a reveals a distinct separation between coniferous, mixedwood and broadleaf dominated stands in the Boreal Shield East. Broadleaf dominated stands had the highest canopy cover (generally > 80%) and the highest GPP (generally 1.0 - 1.3 kgC $m^{-2}yr^{-1}$). Mixedwood stands had high GPP (generally 0.9 - 1.2 kgC $m^{-2}yr^{-1}$) however a wider range in canopy cover as most stands are concentrated between 50 – 95 % cover. Coniferous stands had the largest sampled ranges in both canopy cover and GPP, with the majority of stands having a cover between 20 - 85 % and GPP values between 0.3 - 1.0 kgC $m^{-2}yr^{-1}$. A positive trend between Lidar-derived canopy cover and MODIS GPP is clearly apparent within coniferous stands, while no trend is apparent within broadleaf or mixedwood stands.

Figure 3 provides insight to the drivers of GPP by displaying the relationship between canopy cover and MAT. The relationship between Lidar-derived canopy cover and MAT was only statistically significant in the Boreal Shield East (r = 0.68, p < 0.05, Fig. 3b), where the sampled range of MAT was highest, and the Boreal Cordillera (r = 0.58, p < 0.01, Fig. 3e). Similarly to GPP, the 90 – 100 % cover group in the Boreal Shield East had a higher mean MAT than any other sampled cover group across all ecozones. The relationship between Lidar-derived canopy cover and TAP was not significant in any ecozone.

3.2 Canopy height

Table 2 presents the correlation coefficients, slopes and modified *t*-test results for the relationship between the 95th height percentile and MODIS GPP using a distance interval of 10 km, while Figure 4 displays the relationship as a series of boxplots. The effective sample sizes were relatively similar to Table 1, with the exception of a large increase in the Boreal Cordillera (54.38 to 100.19) and a large decrease in the Boreal Shield West (57.92 to 26.45). Similarly to Lidar-derived cover, changing the distance interval had no effect on the acceptance or rejection of the null hypothesis ($\alpha = 0.05$). The level of significance did change from $p < 0.01$ to 0.001 when the distance was increased from 5 km to 10 km in the Boreal Cordillera. Correlation coefficients were significant in the Boreal Shield East ($r = 0.49$, $p < 0.05$, Fig. 4b) and West ($r = 0.47$, $p < 0.05$, Fig. 4c), the Boreal Cordillera ($r = 0.33$, $p < 0.001$, Fig. 4e), Taiga Plains ($r = 0.59$, $p < 0.05$, Fig. 4g) and Taiga Shield East ($r = 0.45$, $p < 0.05$, Fig. 4f). With the exception of the Boreal Shield West and Hudson Plains, the correlation coefficients between Lidar-derived canopy height and MODIS GPP were lower in each ecozone than for Lidar-derived canopy cover. The majority of stands were concentrated into relatively few height bins compared to canopy cover, with nearly 75 % of the stands in the Boreal Shield East (Fig. 4b) between 9-15 m. The Taiga Plains (Fig. 4g) contained the tallest stands, while few tall stands were sampled in the Taiga Shield East (Fig. 4f) or Hudson Plains (Fig. 5h). Approximately 4 % of stands in the Boreal Shield East had a 95th height percentile above 18 m. Most of these regionally tall stands in the Boreal Shield East are dominated by broadleaf and mixedwood forest types, with coniferous stands reaching a maximum Lidar-derived height near 18 m (Fig. 4a). Compared to the link between Lidar-derived canopy cover and MODIS GPP, the link between the 95th height percentile and MODIS GPP is not as linear, which is apparent by comparing the Boreal Shield East scatterplots (Fig. 2a vs. Fig. 4a). The most notable trend in Fig. 4a is that the maximum sampled height derived from Lidar increases as GPP increases.

3.3 Structural complexity

The relationship between the CV of return heights and MODIS GPP is more complex than percent cover above 2 m or the 95th height percentile. Figure 5a displays the relationship between the CV and MODIS GPP in the Boreal Shield East, with points shaded according to dominant forest type. At low levels of MODIS GPP, the range of sampled CV values was narrow and centered near 0.4. As GPP increases, the range of sampled CV values became wider but remained centered near 0.4. Broadleaf dominated stands generally had the lowest CV, while mixedwood and coniferous stands had a larger range in CV than broadleaf stands.

Figure 5b displays the relationship between the CV of return heights and MODIS GPP for coniferous cells shaded by the 95th height percentile. Short stands tended to have lower CV values than taller stands with similar GPP and the CV of short stands decreased slightly as GPP increased. Taller stands had a wider range of CV values than short stands, and the maximum sampled CV for tall stands increased as GPP increased.

4. Discussion

4.1 Canopy cover

Strong links between Lidar-derived canopy cover and satellite-derived GPP in the boreal are anticipated for two reasons: 1) more productive sites can support a higher density of trees with more dense canopies; and, 2) canopy cover relates to the amount of foliage, which is a key driver of productivity (Schulze et al. 2002). The strength of the relationship between Lidar-derived canopy cover and MODIS GPP across ecozones largely depended on the sampled range of MAT, as temperature is the main climatic driver of productivity in Canadian boreal forests (Churkina and Running 1998; Boisvenue and Running 2006). The largest gradient in MAT occurred in the Boreal Shield East, with cold temperatures limiting the productivity and observed stand density in northern coniferous forests compared to southern broadleaf forests. The observed differences in Lidar-derived canopy cover between forest types in the Boreal Shield East is likely caused by this strong latitudinal gradient, as forest type transitions along with temperature from broadleaf dominated stands in the south to coniferous dominated stands in the north. To investigate the differences in structure across forest types, forest stands under similar site conditions would need to be isolated to remove this latitudinal effect.

While temperature is a main limiting factor of productivity in the Canadian boreal, productivity is fundamentally restricted by the amount of foliage that is absorbing solar radiation (Schulze et al. 2002). The MODIS GPP algorithm accounts for the amount of absorbed solar radiation with the MODIS FPAR product, explaining why MODIS GPP correlates more closely to Lidar-derived canopy cover within most ecozones than temperature data alone. In addition, as the MODIS FPAR product is essentially measuring foliage amounts, FPAR relates directly to canopy cover.

GPP can vary between stands with similar canopy cover values if differences exist in LUE, received solar radiation or the fraction of the canopy that is composed of foliage (Fig. 6a). Productivity can also vary as a function of stand age and successional stage as younger stands are often more productive than older stands (Ryan et al. 1997).

The lack of statistically significant relationships between Lidar-derived canopy cover and TAP are in agreement with past studies showing temperature, not precipitation, to be the primary factor limiting growth in the boreal (Churkina and Running 1998). If precipitation does play a role in determining canopy cover in the boreal, it would be obscured by the strong latitudinal effects in this analysis.

4.2 Canopy height

The correlations between the 95th height percentile and MODIS GPP highlight the importance of successional stage and stand age in shaping structure in Canadian boreal forests. Stand-replacing disturbances are the main determinant of age, and therefore height, in the boreal (Kurz and Apps 1999; Bond-Lamberty et al. 2007; Amiro et al. 2009), explaining why Lidar-derived stand height was not linked as strongly to MODIS GPP as Lidar-derived canopy cover in all but the Boreal Shield West and Hudson Plains. Productivity affects stand height by determining the rate of growth between disturbances and restricting growth in the prolonged absence of disturbance in low productivity sites (Boucher et al. 2006). The relationship between the 95th height percentile and MODIS GPP in the Boreal Shield East likely provides insights to the effects of both productivity and age on forest structure (Fig. 6b). We expect that relatively young stands were sampled across a wide range of MODIS GPP, explaining why the minimum sampled stand height remained relatively constant as GPP increased. Alternatively, the maximum sampled 95th height percentile increased along with MODIS GPP, as we expect growth to be faster and less restricted by resources at high levels of GPP. Therefore, stands can become taller in the prolonged absence of disturbance on more productive sites. It should be noted that stand height will not continuously increase with time since stand-replacing disturbance, as the transition from deciduous to coniferous dominance and non-stand-replacing disturbances can reduce stand height (Paré and Bergeron 1995; Brassard et al. 2008) and stands will not grow indefinitely.

The finding that most coniferous stands reach a maximum 95th height percentile around 18 m in the Boreal Shield East corresponds well to other studies of forest structure in the Boreal Shield (Paré and Bergeron 1995; Brassard et al. 2008). Higher productivity in the southern portion of the ecozone and tall broadleaf species such as trembling aspen allow mixedwoods and broadleaf stands to grow taller than sampled coniferous stands (Paré and Bergeron 1995; Brassard et al. 2008).

4.3 Structural complexity

Successional stage and age also play an important role in determining the structural complexity of forests. We expect that the range of sampled CV values became wider in the Boreal Shield East as GPP increased because of several competing factors (Fig. 6c). First, we expect that fewer young stands were sampled in cells with low GPP compared to cells with high GPP, as growth rates are likely slower where GPP is low, requiring more time for stands to reach five meters in height (i.e., the minimum height considered in this analysis). The inclusion of younger stands at higher levels of GPP could explain why the CV of return height in short stands decreases as GPP increases. Canopy gaps, uneven-aged structure and less dense vegetation in mature, low productivity stands will generally result in more complex forest structures than in young, highly productive stands. Alternatively, maximum tree dimensions are less restricted on highly productive sites and stands can reach an uneven-aged structure faster (Boucher et al. 2006; Larson et al. 2008). Therefore, we expect that mature forest stands will be more structurally complex on high productivity sites than low productivity sites. As a result, the differences between the structural complexities of young and mature stands appears to become greater as GPP increases.

The spherical shape of broadleaf crowns and the greater height of the sampled broadleaf stands in the Boreal Shield East results in generally low CV values for broadleaf dominated stands. The presence of multi-aged and multi-species canopies in mixedwood stands is the expected cause of higher CV values for many mixedwood stands compared to broadleaf stands. There was a wider range in sampled height for mixedwood stands than broadleaf stands, which we expect represents various stages of succession, resulting in a wider range of sampled CV values for mixedwood stands.

4.4 Considerations

Several factors must be considered when analyzing the results of this analysis. We compared a ten-year average of MODIS GPP, which acts as a long-term indicator of forest productivity, to a single snapshot in time of forest structure from airborne Lidar data. As most sampled stands are older than ten years and have varying disturbance histories, productivity over the most recent ten years would only reflect part of the observed stand structure. To better quantify the relationship between productivity and forest structure, we must account for disturbance history, successional stage and stand age. To do so, we attempted to restrict this study to mature unmanaged forests, however the presence of short stands in highly productive forests suggests that we were unable to remove all young stands from the analysis. While management activity is low in most northern boreal forests (Andrew et al. 2012), natural disturbance is a fundamental component of the ecosystem, yet it is infeasible to monitor in its entirety. As a result we accounted for time since disturbance using height as an indicator of age within stands of similar GPP.

Additionally, it must be noted that the swath width of the products generated from the Lidar transects (400m) were narrower than a single MODIS cell (1km), preventing the structure across entire MODIS cells from being measured. The average MODIS cell in this analysis contained 461 Lidar plots, which accounts for approximately 29% of the area of a single MODIS cell. Therefore, the forest stands sampled with Lidar may not accurately represent the productivity of an entire cell in all instances. This should not be a major issue, as we removed any MODIS cell that was less than 75% forested. We assume that variations in productivity are minimal within each 1-km cell, which may not always be the case as differences in nutrient and water availability as well as varying species and stages of succession may be occurring within a single cell.

Finally, we must consider the small sample size in low productivity forests of the Boreal Shield East when analyzing these results. At low levels of GPP (i.e., < 0.6 kgC $m^{-2}yr^{-1}$) in the Boreal Shield East, we reported shorter stands and a narrower range of CV values. However, only 5.7% of the sampled MODIS cells in the ecozone had a GPP value < 0.6 kgC $m^{-2}yr^{-1}$. It is possible that with increased sampling in low productivity forests we would find taller stands or a wider range in structural complexity.

5. Conclusions

Lidar is an invaluable source of data for studying forest structure that allows for an improved characterization of the relationship between productivity and structure over large areas. By measuring forest structure with Lidar data along gradients of productivity in the Canadian boreal, we found a strong link between satellite-derived GPP estimates and boreal forest structure. While the relationship was strong between MODIS GPP and percent cover above 2 m, the weaker relationships to the 95^{th} height percentile and the CV of return height emphasize the importance of stand age in determining the structure of boreal forests. Our results suggest that projected increases in productivity at high latitudes could lead to increases in canopy cover, but changes in habitats, resource availability and carbon storage could also largely depend on changes in disturbance regimes, as disturbance largely controls stand age in boreal forests. Incorporating disturbance history in Lidar studies of structure is therefore critical to improve our understanding of current forest structure and how structure will be altered by a changing climate.

Acknowledgements

Aspects of this research were undertaken as part of the "EcoMonitor: Northern Ecosystem Climate Change Monitoring" project jointly funded by the Canadian Space Agency (CSA), Government Related Initiatives Program (GRIP) and the Canadian Forest Service (CFS) of Natural Resources Canada. Components of this research were also funded by a NSERC Discovery grant to Coops and a graduate scholarship to Bolton. Christopher Bater (previously of UBC and now with the Government of Alberta) is thanked for his analysis efforts and insights in the development of the forest structural attributes from the Lidar metrics. Chris Hopkinson (previously of Nova Scotia Community College and now with the University of Lethbridge) is thanked for his transect project partnership and his leadership of the national Canadian Consortium for LiDAR Environmental Applications Research (C-CLEAR) which was critical in obtaining the research data used in this study. Trevor Milne of Gaiamatics is thanked for assisting with the development of customized code for processing the long lidar transect files.

References

Amiro, B. D., Cantin, A., Flannigan, M. D., & de Groot, W. J. (2009). Future emissions from Canadian boreal forest fires. *Canadian Journal of Forest Research*, *39*, 383–395.

Amiro, B. D., Stocks, B. J., Alexander, M. E., Flannigan, M. D., & Wotton, B. M. (2001). Fire, climate change, carbon and fuel management in the Canadian boreal forest. *International Journal of Wildland Fire*, *10*, 405–413.

Andersen, H. E. (2009). Using airborne light detection and ranging (LIDAR) to characterize forest stand condition on the Kenai Peninsula of Alaska. *Western Journal of Applied Forestry*, *24*(2), 95–102.

Andrew, M. E., Wulder, M. A., & Coops, N. C. (2012). Identification of *de facto* protected areas in boreal Canada. *Biological Conservation*, *146*, 97–107.

Bergeron, Y. (2000). Species and stand dynamics in the mixed woods of Quebec's southern boreal forest. *Ecology*, *81*(6), 1500–1516.

Bergeron, Y., Flannigan, M., Gauthier, S., Leduc, A., & Lefort, P. (2004). Past, current and future fire frequency in the Canadian boreal forest: implications for sustainable forest management. *Ambio*, *33*(6), 356–360.

Boisvenue, C. & Running, S. W. (2006). Impacts of climate change on natural forest productivity - evidence since the middle of the 20th century. *Global Change Biology*, doi:10.1111/j.1365-2486.2006.01134.x

Bond-Lamberty, B., Peckham, S. D., Ahl, D. E., & Gower, S. T. (2007). Fire as the dominant driver of central Canadian boreal forest carbon balance. *Nature*, *450*, 89–93.

Boucher, D., Gauthier, S., & De Grandpré, L. (2006). Structural changes in coniferous stands along a chronosequence and a productivity gradient in the northeastern boreal forest of Québec. *Écoscience*, *13*(2), 172–180.

Bradford, J. B. & Kastendick, D. N. (2010). Age-related patterns of forest complexity and carbon storage in pine and aspen-birch ecosystems of northern Minnesota, USA. *Canadian Journal of Forest Research*, *40*, 401–409.

Brandt, J. P. (2009). The extent of the North American boreal zone. *Environmental Reviews*, *17*, 101–161.

Brassard, B. W. & Chen, H. Y. H. (2006). Stand structural dynamics of North American boreal forests. *Critical Reviews in Plant Sciences*, *25*, 115–137.

Brassard, B. W., Chen, H. Y. H., Wang, J. R., & Duinker, P. N. (2008). Effects of time since stand-replacing fire and overstory composition on live-tree structural diversity in the boreal forest of central Canada. *Canadian Journal of Forest Research*, *38*, 52–62.

Canadian Forest Service (2010). National Fire Database – Agency Fire Data. Natural Resources Canada, Canadian Forest Service, Northern Forestry Centre, Edmonton, Alberta. http://cwfis.cfs.nrcan.gc.ca/en_CA/nfdb. Accessed 19 September 2011.

Carroll, A. L., Taylor, S. W., Régnière, J. & Safranyik, L. (2003). Effects of climate change on range expansion by the mountain pine beetle in British Columbia. In T. L. Shore, J. E. Brooks, J. E. Stone (Eds.), *Mountain Pine Beetle Symposium: Challenges and Solutions* (pp. 223–232). Victoria: Natural Resources Canada, Canadian Forest Service, Pacific Forestry Centre.

Chen, H. Y. H. & Popadiouk, R. V. (2002). Dynamics of North American boreal mixedwoods. *Environmental Reviews*, *10*, 137–166.

Cheng, R., & Lee, P. (2008). Urban sprawl and other major land use conversions in Ontario's Greenbelt From 1993 to 2007. Global Forest Watch Canada. Edmonton, Alberta. http://www.globalforestwatch.ca/ON-greenbelt-2008/ONgreenbelt-change-GFWC2008_LR.pdf. Accessed 10 December 2011.

Cheng, R., & Lee, P. (2009). Recent (1990-2007) anthropogenic change within the forest landscapes of Nova Scotia. Global Forest Watch Canada. Edmonton, Alberta. http://www.globalforestwatch.ca/change_analysis/NS/GFWC_NS-change-2009_LR_WEB.pdf. Accessed 10 December 2011.

Churkina, G. & Running, S. W. (1998). Contrasting climatic controls on the estimated productivity of global terrestrial biomes. *Ecosystems*, *1*, 206–215.

Clifford, P., Richardson, S. and Hemon, D. (1989). Assessing the significance of the correlation between two spatial processes. *Biometrics, 45*(1), 123–134.

Denman, K. L., Brasseur, G., Chidthaisong, A., Ciais, P., Cox, P. M., Dickinson, R. E., et al. (2007). Couplings between changes in the climate system and biogeochemistry. In: S. Solomon, D. Qin, M. Manning, Z. Chen, M. Marquis, K. B. Averyt, M. Tignor & H. L. Miller (Eds.), *Climate Change 2007: The Physical Science Basis. Contribution of Working Group I to the Fourth Assessment Report of the Intergovernmental Panel on Climate Change* (pp. 499–587). Cambridge, UK and New York, NY: Cambridge University Press.

Dubayah, R. O. & Drake, J. B. (2000). Lidar remote sensing for forestry. *Journal of Forestry*, *98*, 44–46.

Dutilleul, P. (1993). Modifying the t test for assessing the correlation between two spatial processes. *Biometrics, 49*(1), 305–314.

Ecological Stratification Working Group (1995). A national ecological framework for Canada. Centre for Land and Biological Resources Research, Research Branch, Agriculture and Agri-Food Canada. http://sis.agr.gc.ca/cansis/publications/ecostrat/cad_report.pdf. Accessed 1 December 2011.

Fahey, T. J., Woodbury, P. B., Battles, J. J., Goodale, C. L., Hamburg, S. P., Ollinger, S. V., & Woodall, C. W. (2010). Forest carbon storage: ecology, management, and policy. *Frontiers in Ecology and the Environment*, *8*(5), 245–252.

Food and Agriculture Organization (2006). Global Forest Resources Assessment 2005: Progress towards sustainable forest management. Food and Agriculture Organization of the United Nations, Rome. ftp://ftp.fao.org/docrep/fao/008/A0400E/A0400E00.pdf. Accessed 6 December 2011.

Flannigan, M. D., Logan, K. A., Amiro, B. D., Skinner, W. R., & Stocks, B. J. (2005). Future area burned in Canada. *Climatic Change*, *72*, 1–16.

Fortin, M.-J., (1999). Effects of sampling unit resolution on the estimation of spatial autocorrelation, *Écoscience, 6*(4), 636–641.

Fortin, M.-J. & Payette, S. (2002). How to test the significance of the relation between spatially autocorrelated data at the landscape scale: A case study using fire and forest maps. *Écoscience, 9*(2), 213–218.

Frelich, L. E. & Reich, P. B. (1995). Spatial patterns and succession in a Minnesota southern-boreal forest. *Ecological Monographs*, *65*(3), 325–346.

Friedl, M. A., Sulla-Menashe, D., Tan, B., Schneider, A., Ramankutty, N., Sibley, A., & Huang, X. (2010). MODIS Collection 5 global land cover: Algorithm refinements and characterization of new datasets. *Remote Sensing of Environment*, *114*, 168–182.

Gillis, M. D., Omule, A. Y., & Brierley, T. (2005). Monitoring Canada's forests: the National Forest Inventory. *The Forestry Chronicle*, *81*(2), 214–221.

Heinsch, F. A., Zhao, M., Running, S. W., Kimball, J. S., Nemani, R. R., Davis, K. J., et al. (2006). Evaluation of remote sensing based terrestrial productivity from MODIS using regional tower eddy flux network observations. *IEEE Transactions on Geoscience and Remote Sensing*, *44*(7), 1908–1925.

Hopkinson, C., Wulder, M. A., Coops, N. C., Milne, T., Fox, A., & Bater, C. W. (2011). Airborne lidar sampling of the Canadian boreal forest: Planning, execution, and initial processing, *Proceedings of the SilviLaser 2011 Conference, Oct. 16–20* (unpaginated). Hobart, Tasmania, Australia. http://www.iufro.org/download/file/8239/5065/40205-silvilaser2011_pdf. Accessed 15 November 2012.

Houghton, R. A., Hall, F., & Goetz, S. J. (2009). Importance of biomass in the global carbon cycle. *Journal of Geophysical Research*, doi:10.1029/2009JG000935

Jennings, S. B., Brown, N. D., & Sheil, D. (1999). Assessing forest canopies and understorey illumination: canopy closure, canopy cover and other measures. *Forestry*, *72*(1), 59–73.

Kane, V. R., Bakker, J. D., McGaughey, R. J., Lutz, J. A., Gersonde, R. F., & Franklin, J. F. (2010a). Examining conifer canopy structural complexity across forest ages and elevations with LiDAR data. *Canadian Journal of Forest Research*, *40*, 774–787.

Kane, V. R., McGaughey, R. J., Bakker, J. D., Gersonde, R. F., Lutz, J. A., & Franklin, J. F. (2010b). Comparisons between field- and LiDAR-based measures of stand structural complexity. *Canadian Journal of Forest Research*, *40*, 761–773.

Kasischke, E. S., Christensen, N. L., & Stocks, B. J. (1995). Fire, global warming, and the carbon balance of boreal forests. *Ecological Applications*, *5*(2), 437–451.

Kneeshaw, D. & Gauthier, S. (2003). Old growth in the boreal forest: A dynamic perspective at the stand and landscape level. *Environmental Reviews*, *11*, S99–S114.

Kneeshaw, D. D. & Bergeron, Y. (1998). Canopy gap characteristics and tree replacement in the southeastern boreal forest. *Ecology*, *79*(3), 783–794.

Kurz, W. A. & Apps, M. J. (1999). A 70-year retrospective analysis of carbon fluxes in the Canadian forest sector. *Ecological Applications*, *9*(2), 526–547.

Kurz, W. A., Dymond, C. C., Stinson, G., Rampley, G. J., Neilson, E. T., Carroll, A. L., et al. (2008a). Mountain pine beetle and forest carbon feedback to climate change. *Nature*, *452*, 987–990.

Kurz, W. A., Dymond, C. C., White, T. M., Stinson, G., Shaw, C. H., Rampley, G. J., et al. (2009). CBM-CFS3: A model of carbon-dynamics in forestry and land-use change implementing IPCC standards. *Ecological Modelling*, *220*, 480–504.

Kurz, W. A., Stinson, G., & Rampley, G. J. (2008b). Could increased boreal forest ecosystem productivity offset carbon losses from increased disturbances? *Phil. Trans. R. Soc. B.*, doi:10.1098/rstb.2007.2198

Larson, A. J., Lutz, J. A., Gersonde, R. F., Franklin, J. F., & Hietpasi, F. F. (2008). Potential site productivity influences the rate of forest structural development. *Ecological Applications*, *18*(4), 899–910.

Lee, P., & Gysbers, J. D. (2008). Recent anthropogenic changes within the inland temperate rainforest of British Columbia: Interim report. Global Forest Watch Canada. Edmonton, Alberta. http://www.globalforestwatch.ca/change_analysis/BC/GFWC_change-BC-INTERIM_lowres.pdf. Accessed 10 December 2011.

Lefsky, M. A., Cohen, W. B., Parker, G. G., & Harding, D. J. (2002). Lidar remote sensing for ecosystem studies. *BioScience*, *52*(1), 19–30.

Lefsky, M. A., Hudak, A. T., Cohen, W. B., & Acker, S. A. (2005). Patterns of covariance between forest stand and canopy structure in the Pacific Northwest. *Remote Sensing of Environment*, *95*, 517–531.

Lim, K., Treitz, P., Wulder, M. A., St-Onge, B., & Flood, M. (2003). LiDAR remote sensing of forest structure. *Progress in Physical Geography*, *27*(1), 88–106.

Mac Nally, R., Parkinson, A., Horrocks, G., Conole, L., & Tzaros, C. (2001). Relationships between terrestrial vertebrate diversity, abundance and availability of coarse woody debris on south-eastern Australian floodplains. *Biological Conservation*, *99*, 191–205.

Magnussen, S. & Boudewyn, P. (1998). Derivations of stand heights from airborne laser scanner data with canopy-based quantile estimators. *Canadian Journal of Forest Research*, *28*, 1016-1031.

Masek, J. G., Cohen, W. B., Leckie, D., Wulder, M. A., Vargas, R., de Jong, B., et al. (2011). Recent rates of forest harvest and conversion in North America. *Journal of Geophysical Research*, doi:10.1029/2010JG001471

McElhinny, C., Gibbons, P., Brack, C., & Bauhus, J. (2005). Forest and woodland stand structural complexity: Its definition and measurement. *Forest Ecology and Management*, *218*(1–3), 1–24.

McGaughey, R. J. (2012). FUSION/LDV: Software for LIDAR data analysis and visualization. Pacific Northwest Research Station, Forest Service, United States Department of Agriculture.
http://forsys.cfr.washington.edu/fusion/FUSION_manual.pdf. Accessed 5 September 2011.

Mesinger, F., DiMego, G., Kalnay, E., Mitchell, K., Shafran, P. C., Ebisuzaki, W., et al. (2006). North American Regional Reanalysis. *Bulletin of the American Meteorological Society*, *87*(3), 343–360.

Monteith, J. L. (1972). Solar radiation and productivity in tropical ecosystems. *Journal of Applied Ecology*, *9*(3), 747–766.

Morsdorf, F., Kötz, B., Meier, E., Itten, K. & Allgöwer, B. (2006). Estimation of LAI and fractional cover from small footprint airborne laser scanning data based on gap fraction. *Remote Sensing of Environment*, *104*, 50–61.
Myneni, R., Knyazikhin, Y., & Shabanov, N. (2011). Leaf area index and fraction of absorbed PAR products from Terra and Aqua MODIS sensors: analysis, validation, and refinement. In B. Ramachandran, C. O. Justice, & M. J. Abrams (Eds.), *Land remote sensing and global environmental change* (pp. 603–633). New York: Springer.
Næsset, E. (2004). Practical large-scale forest stand inventory using a small-footprint airborne scanning laser. *Scandinavian Journal of Forest Research*, *19*(2), 164–179.
Pan, Y., Birdsey, R. A., Fang, J., Houghton, R., Kauppi, R. E., Kurz, W. A., et al. (2011). A large and persistent carbon sink in the world's forests. *Science*, *333*, 988–993.
Paré, D. & Bergeron, Y. (1995). Above-ground biomass accumulation along a 230-year chronosequence in the southern portion of the Canadian boreal forest. *Journal of Ecology*, *83*(6), 1001–1007.
Parry, M., Canziani, O., Palutikof, J., Adger, N., Aggarwal, P., Agrawala, S., et al. (2007). Technical Summary. In M. L. Parry, O. F. Canziani, J. P. Palutikof, P. J. van der Linden & C. E. Hanson (Eds.), *Climate Change 2007: Impacts, Adaptation and Vulnerability. Contribution of Working Group II to the Fourth Assessment Report on the Intergovernmental Panel on Climate Change* (pp. 23–78). Cambridge, UK: Cambridge University Press.
R Development Core Team (2009). R: A language and environment for statistical computing. R Foundation for Statistical Computing, Vienna, Austria. http://www.R-project.org. Accessed 15 November 2012.
Rosenberg, M. S. & Anderson, C. D. (2011). PASSaGE: Pattern analysis, spatial statistics and geographic exegesis. Version 2. *Methods in Ecology and Evolution, 2*(3), 229–232.
Running, S. W., Nemani, R., Heinsch, F. A., Zhao, M., Reeves, M., & Hashimoto, H. (2004). A continuous satellite-derived measure of global terrestrial primary production. *BioScience*, *54*(6), 547–560.
Ryan, M. G., Binkley, D., & Fownes, J. H. (1997). Age-related decline in forest productivity: pattern and process. *Advances in Ecological Research*, *27*, 213–262.
Safranyik, L., Carroll, A. L., Régnière, J., Langor, D. W., Riel, W. G., Shore, T. L., et al. (2010). Potential for range expansion of mountain pine beetle into the boreal forest of North America. *The Canadian Entomologist*, *142*(5), 415–442.
Schulze, E. D., Beck, E., & Müller-Hohenstein, K. (2002). *Plant Ecology*. Berlin: Springer-Verlag.
Solberg, S., Næsset, E., Hanssen, K. H., & Christiansen, E. (2006). Mapping defoliation during a severe insect attack on Scots pine using airborne laser scanning. *Remote Sensing of Environment*, *102*(3-4), 364–376.
Spies, T. A. (1998). Forest structure : A key to the ecosystem. *Northwest Science*, *72*(2), 34–39.
Stanojevic, Z., Lee, P., & Gysbers, J. D. (2006a). Recent anthropogenic changes within the Boreal Plains ecozone of Saskatchewan and Manitoba: Interim report. Global Forest Watch Canada. Edmonton, Alberta. http://www.globalforestwatch.ca/change_analysis/change-analysis-SKMB-150dpi.pdf. Accessed 10 December 2011.
Stanojevic, Z., Lee, P., & Gysbers, J. D. (2006b). Recent anthropogenic changes within the Northern Boreal, Southern Taiga, and Hudson Plains Ecozones of Québec. Global Forest Watch Canada. Edmonton, Alberta. http://www.globalforestwatch.ca/change_analysis/change-analysis-QC-150dpi.pdf. Accessed 10 December 2011.
Statistics Canada (2010). Road Network File, Reference Guide. Statistics Canada, Ottawa, Ontario. http://www.statcan.gc.ca/pub/92-500-g/92-500-g2010001-eng.pdf. Accessed 22 November 2011.
Stinson, G., Kurz, W. A., Smyth, C. E., Neilson, E. T., Dymond, C. C., Metsaranta, J. M., et al. (2011). An inventory-based analysis of Canada's managed forest carbon dynamics, 1990 to 2008. *Global Change Biology*, *17*, 2227–2244.
Stocks, B. J., Mason, J. A., Todd, J. B., Bosch, E. M., Wotton, B. M., Amiro, B. D., et al. (2002). Large forest fires in Canada, 1959–1997. *Journal of Geophysical Research*, doi:10.1029/2001JD000484
Tanabe, S., Toda, M. J., & Vinokurova, A. V. (2001). Tree shape, forest structure and diversity of drosophilid community: Comparison between boreal and temperate birch forests. *Ecological Research*, *16*, 369–385.
Taylor, A. R. & Chen, H. Y. H. (2011). Multiple successional pathways of boreal forest stands in central Canada. *Ecography*, *34*(2), 208–219.
Thornley, J. H. M. & Cannell, M. G. R. (2004). Long-term effects of fire frequency on carbon storage and productivity of boreal forests: a modeling study. *Tree Physiology*, *24*, 765–773.
USDA Forest Service (2003). Field Procedures for the Coastal Alaska Inventory. Pacific Northwest Station. http://www.fs.fed.us/pnw/fia/local-resources/pdf/field_manuals/ak/2003_coak_field_manual.pdf. Accessed 7 May 2012.
Vierling, L. A., Martinuzzi, S., Asner, G. P., Stoker, J., & Johnson, B. R. (2011). LiDAR: providing structure. *Frontiers in Ecology and the Environment*, *9*, 261–262.
Walton, A. (2011). Provincial-Level Projection of the Current Mountain Pine Beetle Outbreak: Update of the infestation projection based on the 2010 Provincial Aerial Overview of Forest Health and the BCMPB model (year 8). BC Forest Service. http://www.for.gov.bc.ca/ftp/hre/external/!publish/web/bcmpb/year8/BCMPB.v8.BeetleProjection.Update.pdf. Accessed 23 April 2012.

Wehr, A. & Lohr, U. (1999). Airborne laser scanning—an introduction and overview. *ISPRS Journal of Photogrammetry and Remote Sensing*, *54*, 68–82.

Wulder, M. A., Bater, C. W., Coops, N. C., Hilker, T., & White, J. C. (2008a). The role of LiDAR in sustainable forest management. *The Forestry Chronicle*, *84*(6), 807–826.

Wulder, M. A., Campbell, C., White, J. C., Flannigan, M., & Campbell, I. D. (2007). National circumstances in the international circumboreal community. *Forestry Chronicle*, *83*(4), 539–556.

Wulder, M. A., White, J. C., Cranny, M. M., Hall, R. J., Luther, J. E., Beaudoin, A., et al. (2008b). Monitoring Canada's forests. Part 1: Completion of the EOSD land cover project. *Canadian Journal of Remote Sensing*, *34*(6), 549–562.

Wulder, M. A., White, J. C., Bater, C. W., Coops, N. C., Hopkinson, C. & Chen, G. (2012). Lidar plots—a new large-area data collection option: context, concepts, and case study. *Canadian Journal of Remote Sensing*, doi:10.5589/m12-049

Zhao, M., Heinsch, F. A., Nemani, R. R., & Running, S. W. (2005). Improvements of the MODIS terrestrial gross and net primary production global data set. *Remote Sensing of Environment*, *95*, 164–176.

Zhao, M. & Running, S. W. (2010). Drought-induced reduction in global terrestrial net primary production from 2000 through 2009. *Science*, *329*, 940–943.

Zimble, D. A., Evans, D. L., Carlson, G. C., Parker, R. C., Grado, S. C., & Gerard, P. D. (2003). Characterizing vertical forest structure using small-footprint airborne lidar. *Remote Sensing of Environment*, *87*, 171–182.

Figures and Tables

Fig. 1 a) Path of 34 small-footprint Lidar transects flown by CFS in 2010 b) Average annual MODIS GPP from 2001-2010 c) Percent of each 1-km MODIS cell classified as forest by the EOSD d) Presence or absence of fire, roads or anthropogenic change within each 1-km MODIS cell e) Selected mature unmanaged MODIS cells shaded by Lidar-derived canopy cover f) Number of MODIS cells selected for analysis within each boreal ecozone

Fig. 2 Relationship between percent cover above 2 m and MODIS GPP for a) Boreal Shield East (scatterplot), shaded by dominant forest type b) Boreal Shield East (boxplot) c) Boreal Shield West d) Boreal Plains e) Boreal Cordillera f) Taiga Shield East g) Taiga Plains h) Hudson Plains. The number above each bin corresponds to the number of samples within the bin

Fig. 3 Relationship between percent cover above 2 m and MAT for a) Boreal Shield East (scatterplot), shaded by dominant forest type b) Boreal Shield East (boxplot) c) Boreal Shield West d) Boreal Plains e) Boreal Cordillera f) Taiga Shield East g) Taiga Plains h) Hudson Plains. The number above each bin corresponds to the number of samples within the bin

Fig. 4 Relationships between 95^{th} height percentile and MODIS GPP for a) Boreal Shield East (scatterplot), shaded by dominant forest type b) Boreal Shield East (boxplot) c) Boreal Shield West d) Boreal Plains e) Boreal Cordillera f) Taiga Shield East g) Taiga Plains h) Hudson Plains. The number above each bin corresponds the number of samples within the bin

Fig. 5 a) Relationship between the CV of return height and MODIS GPP in the Boreal Shield East, shaded by a) dominant forest type b) the 95^{th} height percentile (coniferous dominated stands only)

Fig. 6 Schematic representations of the observed relationships in the Boreal Shield East between MODIS GPP and a) percent cover above 2 m b) 95th height percentile c) CV of return height

Table 1 The correlation coefficients, slopes and modified t-test results for the relationship between percent cover above 2 m (*X*) and MODIS GPP, MAT and TAP (*Y*). A distance interval of 10 km was used to calculate the effective sample size. Slopes are only displayed for the statistically significant relationships (α = 0.05).

Ecozone	Variable	Sample Size	*k*	Effective Sample Size	r	Slope*100
Boreal Shield E.	GPP	1809	257	12.82	0.74**	0.71
	MAT			11.77	0.68*	6.66
	TAP			11.35	-0.51	
Boreal Shield W.	GPP	842	121	57.92	0.27*	0.18
	MAT			43.01	0.22	
	TAP			65.16	-0.04	
Boreal Plains	GPP	145	112	50.62	0.44**	0.22
	MAT			78.52	0	
	TAP			51.56	-0.11	
Boreal Cordillera	GPP	1488	84	54.38	0.58***	0.36
	MAT			27.55	0.58**	3.07
	TAP			81.49	0.19	
Taiga Shield E.	GPP	465	112	15.14	0.57*	0.51
	MAT			15.34	0.41	
	TAP			11.94	0.49	
Taiga Plains	GPP	701	144	17.23	0.70**	0.46
	MAT			12.72	0.46	
	TAP			16.11	0.37	
Hudson Plains	GPP	136	84	9.98	0.47	
	MAT			13.74	0.29	
	TAP			22.08	-0.25	

* < 0.05, ** < 0.01, *** < 0.001, level of significance

Table 2 The correlation coefficients, slopes and modified t-test results for the relationship between the 95th height percentile (X) and MODIS GPP (Y). A distance interval of 10 km was used to calculate the effective sample size. Slopes are only displayed for the statistically significant relationships ($\alpha = 0.05$).

Ecozone	Sample Size	*k*	Effective Sample Size	r	Slope*100
Boreal Shield E.	1809	257	19.35	0.49*	2.99
Boreal Shield W.	842	121	26.45	0.47*	1.45
Boreal Plains	145	112	40.47	0.12	
Boreal Cordillera	1488	84	100.19	0.33***	0.89
Taiga Shield E.	465	112	24.03	0.45*	3.34
Taiga Plains	701	144	16.72	0.59*	1.51
Hudson Plains	136	84	11.10	0.47	

* < 0.05, ** < 0.01, *** < 0.001, level of significance

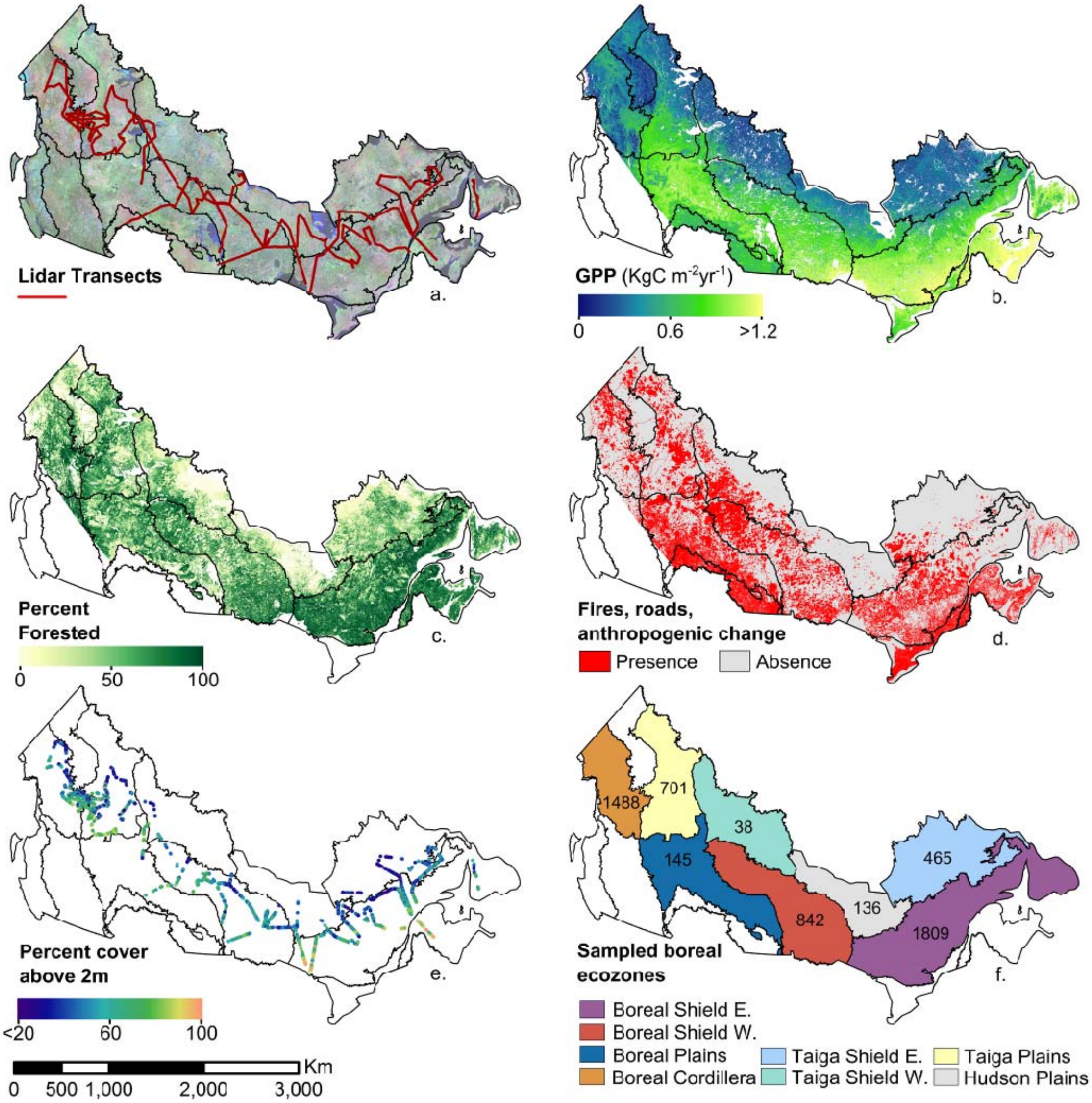

Fig. 1 a) Path of 34 small-footprint Lidar transects flown by CFS in 2010 b) Average annual MODIS GPP from 2001-2010 c) Percent of each 1-km MODIS cell classified as forest by the EOSD d) Presence or absence of fire, roads or anthropogenic change within each 1-km MODIS cell e) Selected mature unmanaged MODIS cells shaded by Lidar-derived canopy cover f) Number of MODIS cells selected for analysis within each boreal ecozone

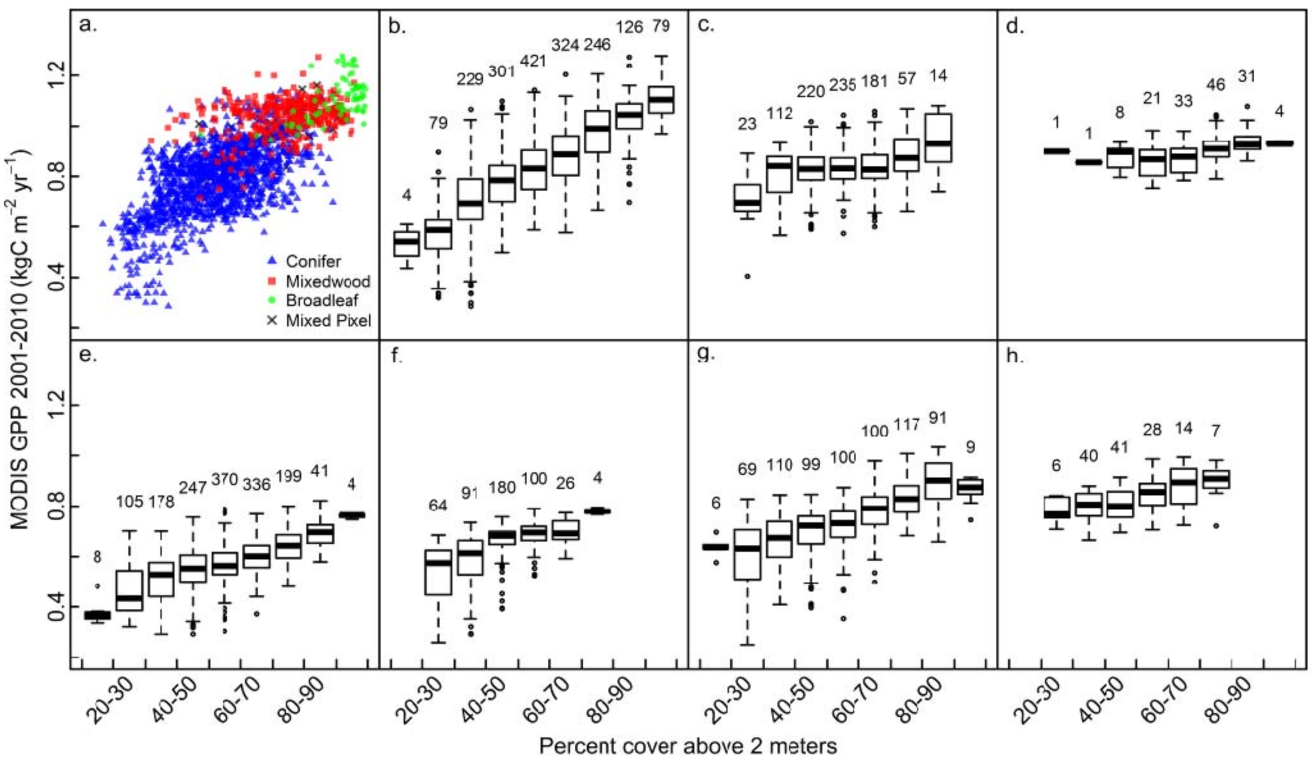

Fig. 2 Relationship between percent cover above 2 m and MODIS GPP for a) Boreal Shield East (scatterplot), shaded by dominant forest type b) Boreal Shield East (boxplot) c) Boreal Shield West d) Boreal Plains e) Boreal Cordillera f) Taiga Shield East g) Taiga Plains h) Hudson Plains. The number above each bin corresponds to the number of samples within the bin

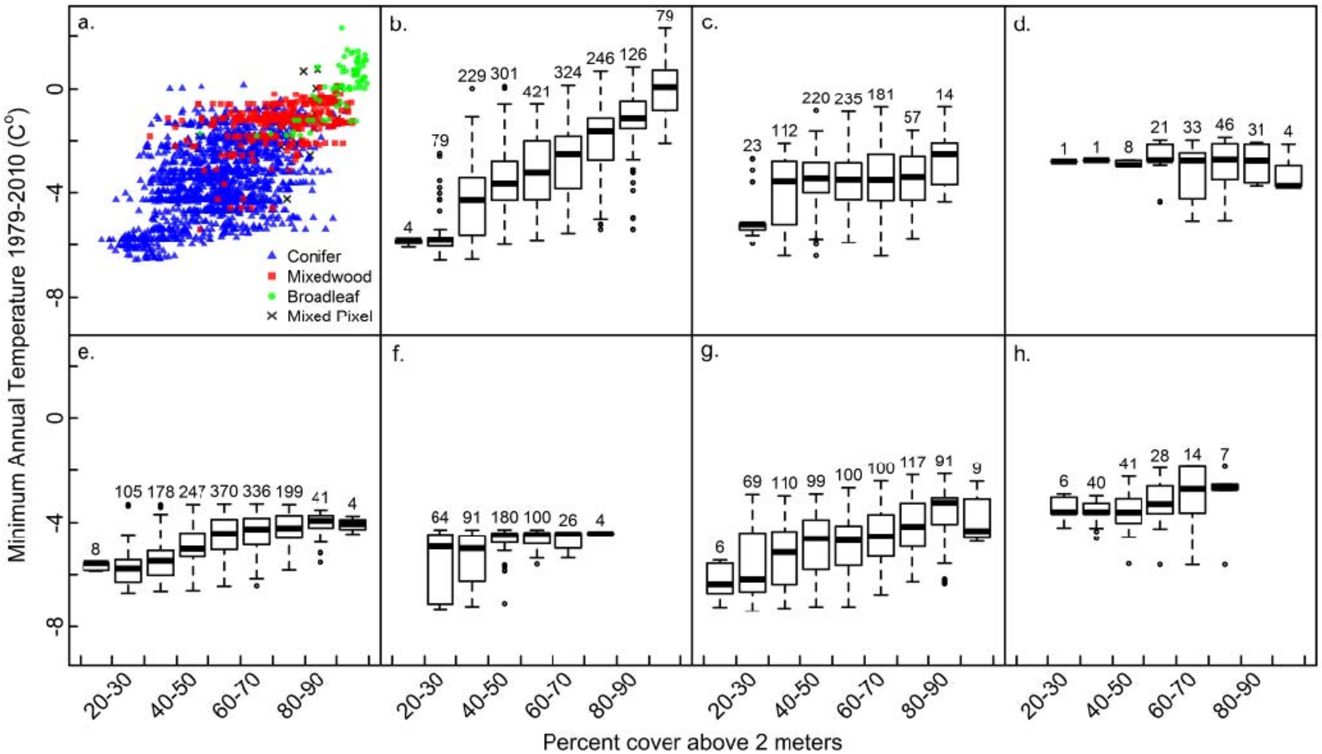

Fig. 3 Relationship between percent cover above 2 m and MAT for a) Boreal Shield East (scatterplot), shaded by dominant forest type b) Boreal Shield East (boxplot) c) Boreal Shield West d) Boreal Plains e) Boreal Cordillera f) Taiga Shield East g) Taiga Plains h) Hudson Plains. The number above each bin corresponds to the number of samples within the bin

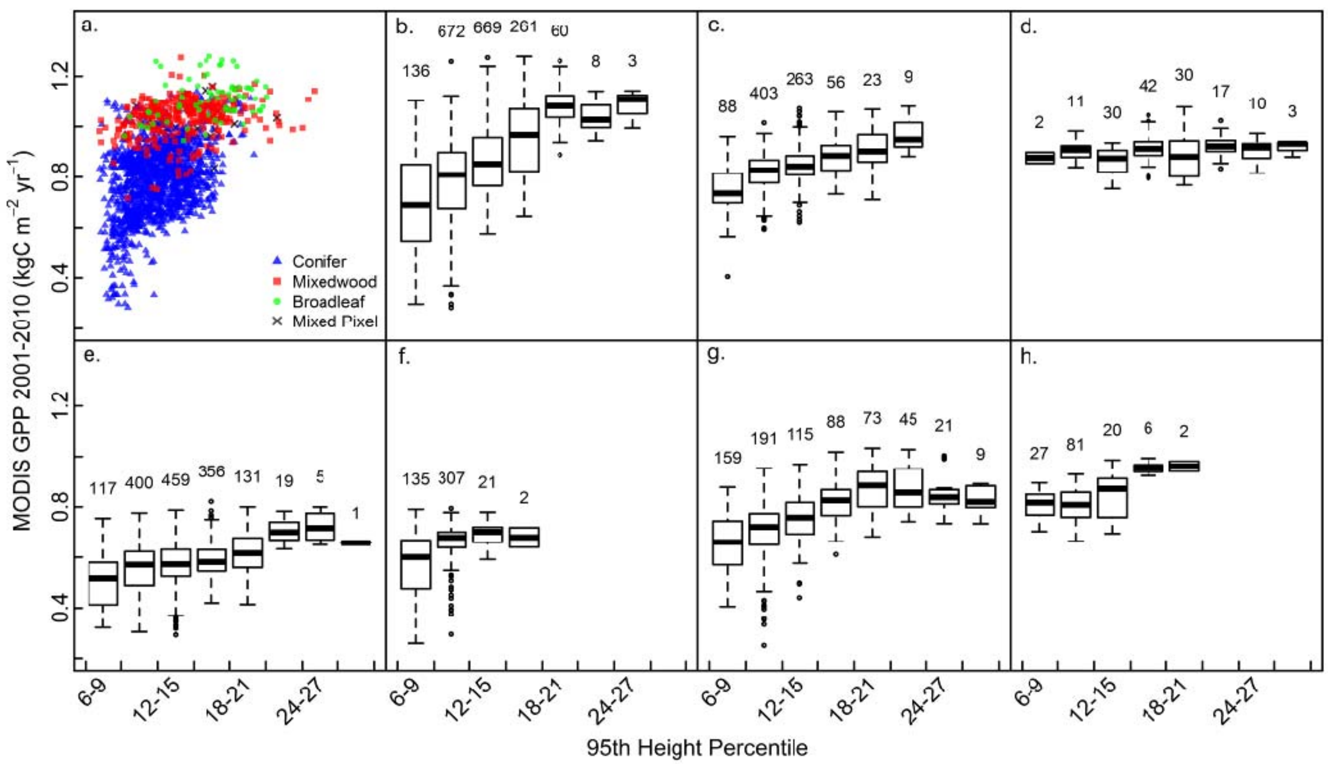

Fig. 4 Relationships between 95th height percentile and MODIS GPP for a) Boreal Shield East (scatterplot), shaded by dominant forest type b) Boreal Shield East (boxplot) c) Boreal Shield West d) Boreal Plains e) Boreal Cordillera f) Taiga Shield East g) Taiga Plains h) Hudson Plains. The number above each bin corresponds the number of samples within the bin

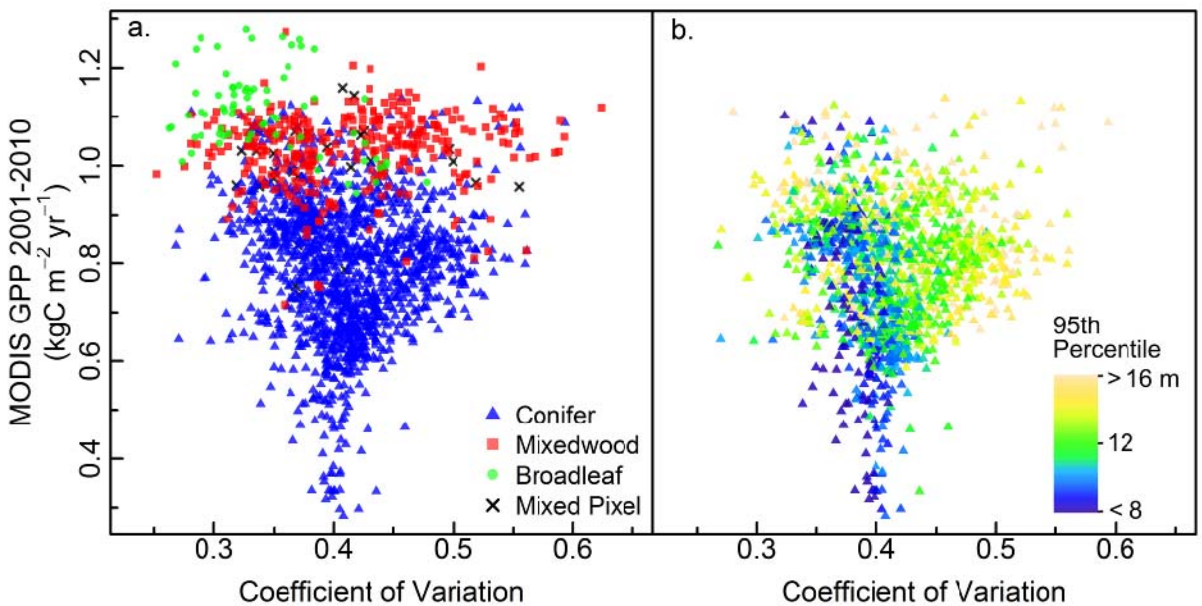

Fig. 5 a) Relationship between the CV of return height and MODIS GPP in the Boreal Shield East, shaded by a) dominant forest type b) the 95th height percentile (coniferous dominated stands only)

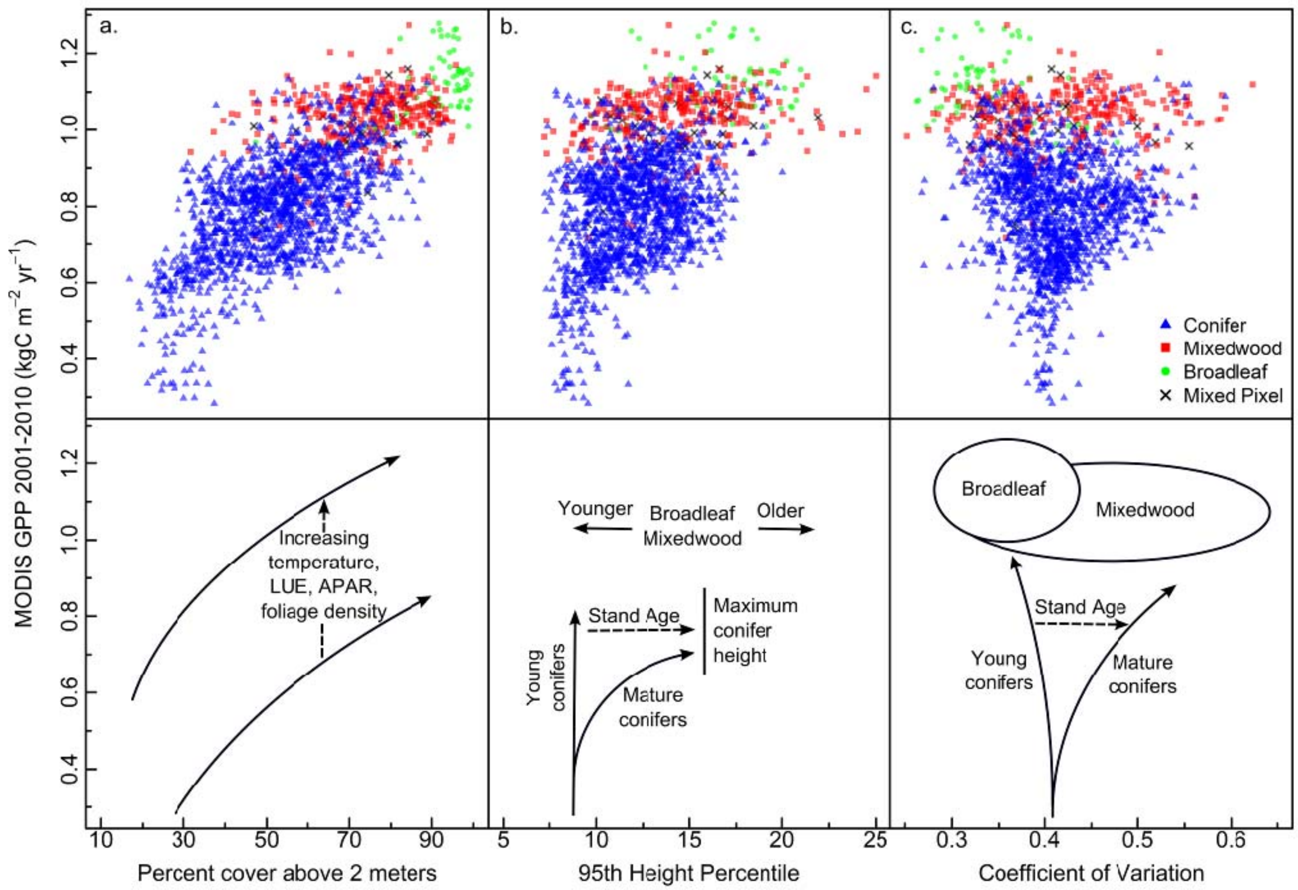

Fig. 6 Schematic representations of the observed relationships in the Boreal Shield East between MODIS GPP and a) percent cover above 2 m b) 95th height percentile c) CV of return height